



Mesoporous zeolites as enzyme carriers: Synthesis, characterization, and application in biocatalysis

Sharon Mitchell, Javier Pérez-Ramírez*

Institute for Chemical and Bioengineering, Department of Chemistry and Applied Biosciences, ETH Zürich, HCI E 125, Wolfgang-Pauli-Strasse 10, CH-8093 Zürich, Switzerland

ARTICLE INFO

Article history:

Available online 16 November 2010

Keywords:

Mesoporous zeolites
Hierarchical porosity
Silanization
Enzyme
Biocatalysis

ABSTRACT

We study the application of hierarchical ZSM-5 zeolites, combining micropores and intracrystalline mesopores, as carriers for lipase enzymes compared with purely microporous ZSM-5 and mesoporous MCM-41. Strategies to improve enzyme immobilization by modification of the support porosity and surface properties (e.g. by reaction with organosilane, or by treatment with the enzyme cross-linking agent glutaraldehyde) are also reported. Spectroscopic screening of catalyst activity and recyclability for the aqueous phase hydrolysis of *p*-nitrophenyl esters, permits evaluation of the influence of support properties and immobilization conditions on the performance of the resulting biocatalysts. An excellent correlation is observed between the mesopore surface area, the enzyme uptake, and the corresponding biocatalyst activity, demonstrating the functional character of mesopores in hierarchical zeolites. Modification of the mesopore walls prior to enzyme immobilization is essential to attain an active and recyclable biocatalyst. Enzymes immobilized on purely inorganic supports exhibit rapid loss of activity attributed to enzyme leaching. Despite the high mesopore surface area of surface-functionalized MCM-41, the mono-dimensionality of the mesopores results in restricted accessibility and a reduced enzyme uptake. In comparison, the interconnected mesopores of the hierarchical zeolites remain accessible after surface functionalization showing good adsorption properties. Lipase immobilized on thiol-functionalized mesoporous ZSM-5 was found to be the most efficient biocatalyst.

© 2010 Elsevier B.V. All rights reserved.

1. Introduction

In comparison with other ordered mesoporous solids, the capacity of zeolites as carriers for large active species has received little attention. Due to their microporous nature (pore widths not exceeding 2 nm [1]) immobilization is typically confined to the external particle surface resulting in limited uptake and protection of the guest [2,3]. The use of nano-crystallites [4,5] or delaminated zeolites [6] to effectively increase the external surface area of zeolites offers some enhancement in their carrier efficiency. From a practical perspective, however, such strategies are often unfavorable due to the consequential reduction in particle sizes which results in reduced processability.

So far, the capacity of zeolites as carriers for large active species may also be improved by the application of hierarchical zeolites, *i.e.* zeolites with auxiliary mesoporosity. Mesoporous zeolites can be obtained in many different ways (e.g. by templating, controlled crystallization, or demetallation) and the mesopores may have inter- and/or intracrystalline character [7]. Conceptually, hierarchical zeolites were sought after in order to improve

transport properties to catalytically active sites located in the micropores, thus improving their utilization efficiency [7,8]. Apart from increased micropore accessibility, the mesopores present may also act as hosts for larger guest species (e.g. biological, metal complexes, etc.) for application as adsorbents/carriers, offering internal surface areas with tunable accessibility and modifiable properties. The differing functionality was shown by Ryoo and co-workers [9], who exploited the mesopores of hierarchical zeolites prepared by surfactant templating to graft a Pd complex for use in Sonogashira coupling reactions. Recent progress in the preparation of hierarchical zeolites by desilication under alkaline conditions, offers a versatile top-down method for the formation of mesopores in commercially available zeolites [10–12]. The higher Si/Al content permits the obtainment of greater mesoporosity than that achievable by dealumination, while also maintaining a negative framework charge. In addition, due to the increased presence of reactive surface silanol groups following alkaline treatment, common methods for the organic functionalization of the mesopores could also be applicable to tailor their surface properties.

Enzyme-containing biocatalysts are of interest due to the high rate enhancements and degrees of regio-, stereo-, and enantioselectivity which they may exhibit. Industrially the use of enzymes remains relatively low as a consequence of the costs associated with the limited catalytic lifetimes, and due to the narrow range

* Corresponding author. Fax: +41 44 633 1405.

E-mail address: jpr@chem.ethz.ch (J. Pérez-Ramírez).

of operating conditions [13]. Enzyme immobilization is advantageous in the preparation of functional biocatalysts, by facilitating the recovery and reuse of the active component, broadening the range of stable operating conditions, and improving their storage stability (e.g. with respect to autolysis). The first conscious attempt at enzyme immobilization is thought to be that of Michaelis and Ehrenreich in 1908 who immobilized the enzyme invertase on charcoal [14]. Using the same system, this strategy was first transferred to a commercial context by Tate and Lyle in 1944 [15], and other early industrial applications followed in the late 1960s [16,17]. Since then many developments have been made in enzymatic biotransformations, which have been reviewed by numerous articles [18–26]. It is known that the support may also play an important role in enzymatic catalysis through interaction with substrate/product species and by provision of optimal operating environments. Materials with high (accessible) surface areas and which provide a favorable enzyme–support interaction are typically preferred to obtain high loadings of the catalytic species and therefore high associated activities. The interaction between enzyme and support is an important consideration as it may influence the activity and stability of the immobilized enzyme. Many different materials (e.g. organic/inorganic, amorphous/crystalline, porous/nonporous) have been studied in the search for suitable enzyme carriers. Ordered mesoporous silicas (commonly MCM-41, SBA-15, and FSM-16) have received much interest [27–33]. The uniformly sized mesopores are envisioned to provide protected reaction environments for the immobilized species. However, several factors have limited the widespread application of mesoporous silicas as enzyme hosts; their synthesis can be costly and time consuming; they have suffered from rapid enzyme leaching; the pore size of many commonly available mesoporous silicas is too small to accommodate larger enzymes.

The disordered (both in size and/or shape) and interconnected intracrystalline mesopores in certain hierarchical zeolites present an alternative type of mesoporous support, based on a zeolitic framework. Zeolites possess several attributes which are *a priori* attractive for enzyme immobilization. The wide range of framework arrangements [34], variable framework charge, exchangeable counterions, and reactive surface silanol groups provide several routes for optimization of enzyme–support interaction and biocatalyst performance [3,35]. Choice of appropriate surface topology [35], the formation of strong ionic enzyme–support interactions [29] and grafting of various types of functional groups have all yielded improved enzyme uptake and retention by zeolites. In addition, the variable water content of zeolites may act as a source of water essential for enzymatic activity when applied to organic phase catalysis [34]. Furthermore, their high chemical and thermal stability permits use in different operating environments, shaping for industrial scale applications, and catalyst regeneration following enzyme deactivation [4,33].

In this work, we demonstrate the benefits of mesoporous zeolites prepared by desiccation for the immobilization of lipase (triacylglycerol ester hydrolase, EC no. 3.1.1.3). Lipase enzymes are an important class of commercial enzymes as they may be employed in both aqueous and organic media [36]; do not require cofactors; exhibit high enantiomeric selectivity [37]; and have a broad substrate specificity [38]. For comparative purposes, purely microporous ZSM-5 and MCM-41 are studied in parallel. Silanization of the supports with aminopropyltriethoxysilane or mercaptopropyltrimethoxysilane enables comparison of the relative performance of surface-functionalized hierarchical zeolites. Additionally, the effect of glutaraldehyde, a common enzyme cross-linking agent [39], is also investigated. The activity and reusability of the resulting biocatalysts is assessed spectroscopically for the hydrolysis of *p*-nitrophenylesters in aqueous medium.

2. Experimental

2.1. Materials

Commercial ZSM-5 zeolite with a nominal Si/Al ratio of 26 (CBV5524G) was supplied by Zeolyst International in the ammonium form. Two commercially available lipase enzyme powders (AS and AK), extracted from different biological sources, were obtained from Anamo Enzyme Inc. All other reagents including MCM-41 (nominal Si/Al ratio of 39.5) were used as supplied from Sigma Aldrich.

2.2. Preparation of mesoporous zeolites

Alkaline treatment of the parent (P), zeolite (1 g) was undertaken with aqueous sodium hydroxide (0.2 M, 30 cm³) for 30 min at 338 K. The alkaline-treated zeolite (H) was isolated by filtration, washed with distilled water until the emitted filtrate was pH neutral, and dried in an oven overnight. Mild acid washing of the alkaline-treated H zeolite was achieved by dispersion in diluted HCl (0.1 M, 30 cm³) solution for 6 h at 290 K. The washed mesoporous zeolite (HW) was collected by filtration and dried as above. The ammonium form of each zeolite was obtained by dispersion (1 g) in ammonium nitrate solution (0.1 M, 30 cm³) for 6 h. This was repeated three times, the zeolite was collected by filtration and washed with distilled water after each step, and was dried after the third repetition. Finally, the zeolites in the ammonium form were converted to the protonic form by thermal decomposition. Samples were heated to 773 K at 5 K min⁻¹ and held at the ceiling temperature for 5 h.

2.3. Modification of the inorganic supports

Prior to attempted functionalization the zeolites, in the protonic form, were dried at 573 K for 4 h. Reactions with aminopropyltriethoxysilane or mercaptopropyltrimethoxysilane were undertaken in *n*-hexane for 24 h. The amounts used were based on the estimated amount required to achieve a monolayer coverage of 5×10^{18} molecules m⁻² [40], which was calculated (assuming that the reaction was limited to the mesoporous and external surface area) from the values of S_{meso} measured by N₂ adsorption. The amino (N-) and thiol (S-) functionalized products were collected by filtration, washed with *n*-hexane and dried at 373 K. Treatment with glutaraldehyde (G-) was undertaken by stirring the support material in aqueous glutaraldehyde solution (0.5 M). The G-functionalized products were collected by filtration, washed with distilled water and dried at 373 K.

2.4. Enzyme immobilization

Lipase immobilization was achieved by dispersion of the support material (100 mg) in buffered (sodium phosphate, 0.05 M) aqueous enzyme containing (5 cm³, 20 mg cm⁻³ enzyme powder) solution at pH 7. The as-supplied powdered lipase enzymes were dissolved in the sodium phosphate buffer and the insoluble content removed via filtration prior to introduction of the support. An orbital shaker was used to stir the support–enzyme containing solutions for 2 h. The immobilized lipase enzymes were collected by filtration and dried at room temperature. The Bradford assay was used to estimate the variation in enzyme content present in the solution before and after dispersion of the support. Aliquots extracted during immobilization were diluted (dependent on enzyme studied). The diluted enzyme (1 cm³) was added to the Bradford reagent (5 cm³) and the resulting solution was incubated for 10 min prior to measurement of the intensity of the absorbance at 595 nm by UV–vis spectroscopy. Comparison with

the absorbance of standard solutions prepared with pure gamma globulin permitted estimation of the purity of the commercial enzymes.

2.5. Characterization

X-ray diffraction (XRD) was undertaken using a Siemens D5000 diffractometer with Bragg-Brentano geometry and Ni filtered Cu $K\alpha$ radiation ($\lambda = 0.1541$ nm). Data were recorded in the range 5–50 2θ with an angular step size of 0.05° and a counting time of 8 s per step. Transmission electron microscopy (TEM) was carried out in a JEOL JEM-1011 microscope operated at 100 kV. The sample was dispersed from ethanol onto a carbon-coated copper grid which was subsequently dried at room temperature. Energy dispersive X-ray analysis was undertaken using a JEOL JSM-6400 microscope operated at 20 kV. The compositions were averaged over 10 independent sites within each sample. Nitrogen isotherms were measured in a Quantachrome Quadrasorb-SI gas adsorption analyzer at 77 K. Samples were degassed in vacuum at 573 K for 10 h prior to measurement. The BET method was applied to calculate the total surface area, the t -plot method was used to discriminate between micro- and meso-porosity, and the total pore volume was derived from the amount of nitrogen adsorbed at $p/p_0 = 0.98$. *In situ* Fourier transform infrared spectroscopy was carried out in a Thermo Nicolet 5700 spectrometer (Thermo Scientific) using a SpectraTech Collector II diffuse reflectance (DRIFT) accessory equipped with a high-temperature chamber, ZnSe windows, and a mercury cadmium telluride (MCT) detector. Spectra were recorded at 453 K after degasification for 2 h prior to measurement, using KBr (Aldrich, IR spectroscopy grade) treated equivalently as the background. The range $650\text{--}4000\text{ cm}^{-1}$ was covered by co-addition of 32 scans at a nominal resolution of 4 cm^{-1} . Elemental analysis was undertaken by the Micro-laboratory, Laboratory of Organic Chemistry, ETH Zürich. A LECO CHN-900 analyzer was used to determine the C, H, and N content. Thermogravimetry was measured in a Mettler Toledo TGA/SDTA851e microbalance. Analyses were performed in air ($50\text{ cm}^3\text{ min}^{-1}$) ramping the temperature from 303 to 1273 K at 5 K min^{-1} .

2.6. Activity assays

Stock solutions of the *p*-nitrophenol esters (*p*NPEs, 1.2 mM) were prepared in isopropanol (HPLC grade) and stored at 280 K. Assays were undertaken in standard cells with a reaction volume of 10 cm^3 at a constant temperature of 298 K using an orbital shaker to provide external stirring at 200 rpm. Cells were charged with a known amount of biocatalyst. Aqueous phase reactions were undertaken in 4 cm^3 of sodium phosphate buffer solution (0.05 M, pH 6) with 0.75 cm^3 of isopropanol and the reaction was initiated by addition of 0.25 cm^3 of substrate solution. After 30 min of reaction the solid catalyst was removed by filtration. The absorbance was measured in the 250–500 nm range using a Shimadzu UV-2401PC spectrophotometer with 10 mm optical path cells. Standard solutions of known quantities of the *p*NPEs and the *p*NP hydrolysis product were prepared for calibration of the results of activity screening. The degree of conversion achieved during the assay was estimated by comparison of the relative intensities of the absorbance of the *p*NPE substrate and *p*NP product. For each catalytic screening a blank was prepared with no added catalyst to accurately determine the extent of spontaneous hydrolysis in order to distinguish hydrolysis associated with enzymatic catalysis. The activities of the base zeolites and MCM-41 host materials and of the lipase enzymes were studied individually prior to assessment of the activity of the supported enzymes in order to distinguish between the relative activities of each species.

3. Biocatalyst preparation

Biocatalyst preparation may be divided into three separate stages (i) development of mesoporosity in purely microporous zeolites, (ii) organic-modification of the external surface, and (iii) immobilization of lipase enzymes onto unfunctionalized and surface-functionalized supports. The experimental approach and nomenclature followed in this work are summarized in Fig. 1. Specific details were elaborated in Section 2.

3.1. Micro-, meso-, and hierarchically porous supports

The ZSM-5 P zeolite with Si/Al ratio of 26 was desilicated in aqueous NaOH under conditions selected to obtain significant mesoporosity development [41–44]. Results from EDX analysis confirm a decrease in the Si/Al ratio in the H zeolite (Si/Al = 23). Due to the important implications of the mesoporous surface composition (e.g. with respect to support–enzyme interactions) some of the H zeolite was subjected to a further mild acid washing step (HW zeolites). This treatment permits removal of any non-framework aluminum resulting from alkaline treatment and recovery of a composition similar to that of the P zeolite while retaining the level of mesoporosity developed during alkaline treatment [44].

Table 1 summarizes the compositional and textural properties of the zeolites and MCM-41 studied. Similar trends are observed as those previously reported for the alkaline treatment [11] and acid washing [44] of ZSM-5. Comparison of the XRD patterns confirms retention of the MFI framework in both the H and HW zeolites (Supporting Information, Fig. S1). The differing morphological and textural properties of the supports may be observed by comparison of the N_2 adsorption isotherms (Fig. 2) and TEM micrographs (Fig. 3). Consistent with purely microporous materials the P zeolite exhibits type I isotherms with a high uptake at low relative pressures, and a much lower uptake at high relative pressures. The mesoporous surface area, S_{meso} , of $62\text{ m}^2\text{ g}^{-1}$, is thought to be primarily due to contributions arising from inter-crystallite mesoporosity and the external crystal surface, and no significant intra-crystalline mesoporosity was observed by TEM (Fig. 3a). Upon alkaline treatment of P, the generation of mesoporosity is evidenced by changes in the form of the N_2 adsorption isotherms, which exhibit a combination of type I and IV behavior. An increase in S_{meso} from 62 to $153\text{ m}^2\text{ g}^{-1}$, and the total pore volume (V_{pore}) from 0.24 to $0.46\text{ cm}^3\text{ g}^{-1}$ combined with a slight reduction in the micropore volume (V_{micro}) from 0.14 to $0.11\text{ cm}^3\text{ g}^{-1}$ are consistent with mesopore formation [41]. The disordered mesopores formed, which are clearly visible by TEM, have differing shapes and sizes (Fig. 3b). This agrees with previous observations which have shown that desilication results in the formation of interconnected intracrystalline mesopores, well distributed throughout the zeolite crystal [43]. Acid washing resulted in a slightly larger deviation in S_{meso} than previously reported [44] (increasing from 153 to $171\text{ m}^2\text{ g}^{-1}$), which is most likely a consequence of the higher aluminum content present in this sample. In comparison with the zeolites, purely mesoporous MCM-41 (pore diameter 2.5–3 nm) shows a higher nitrogen uptake ($V_{\text{pore}} = 1.15\text{ cm}^3\text{ g}^{-1}$, $S_{\text{meso}} = 927\text{ m}^2\text{ g}^{-1}$) and no detectable microporosity. The isotherm is type IVb isotherm and exhibits a steep rise at $p/p_0 = 0.35$ and adsorption hysteresis at $p/p_0 > 0.42$, as expected [45,46]. TEM confirms the ordered hexagonal arrangement and size uniformity of the mesopores (Fig. 3c).

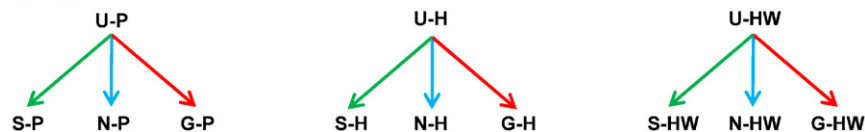
3.2. Modification of support surface properties

Due to its relative simplicity, and to the fewer conformational restrictions imposed, physical adsorption is a common approach for enzyme immobilization on inorganic supports [47]. The lack of a strong covalent link, however, often causes rapid catalyst deac-

1) Mesoporosity development:



2) Organic Modification:



3) Enzyme immobilization:

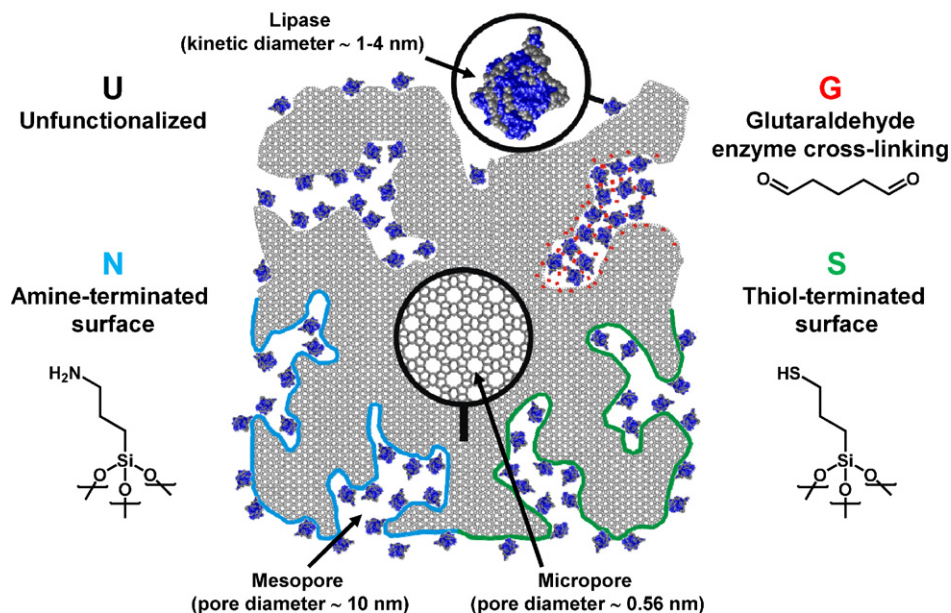


Fig. 1. Summary of the experimental strategy and nomenclature used for immobilization of lipase enzymes on ZSM-5 zeolites with varying surface and textural properties.

tivation as a result of enzyme leaching [48]. For lipase enzymes, improvements of biocatalyst performance have been reported by immobilization on hydrophobic surfaces (e.g. propyltrimethoxysilane or chlorotrimethylsilane) [49,50]. Terminal silanol groups located on the external surface of many (alumino-)silicate based materials are often reactive and may undergo condensation or cross-coupling reactions. For applications as supports such reactivity may be exploited to permit modification of the surface properties in order to enhance the support–enzyme interaction, or to enhance the performance of the support–enzyme complex in a given application.

In order to compare two surfaces of differing functionality ($-\text{NH}_2$ and $-\text{SH}$ terminal groups) and textural properties, the supports were functionalized by reaction with aminopropyltriethoxysilane (N) or mercaptopropyltriethoxysilane (S). These silanization reactions are well characterized [40,51,52], the grafted moieties are of similar size, and have previously been employed to promote enzyme–substrate interactions [53].

Coupling with glutaraldehyde is an alternative strategy commonly used for inter-enzyme (e.g. cross-linked enzyme aggregates) coordination. For mesoporous materials, treatment with glutaraldehyde during immobilization has been reported as an effective approach to reduce the rate of enzyme leaching by effective entrapment of the resulting enzyme aggregates [48]. Pre-treatment of the supports with the polyaldehyde coupling agent has also been reported to give improved enzyme retention [53]. In this work the influence of glutaraldehyde pretreatment (G-) and simultaneous addition during enzyme immobilization (denoted +G) were both studied.

No noticeable changes were observed by XRD following organic modification of the inorganic supports (not shown), indicating that the treatments proceeded with minimal variation in the framework crystallinity and no crystalline impurities were formed. The involvement of the terminal silanol groups on surface silanization is clearly evidenced by infrared spectroscopy (Fig. 4). An increase in the intensity of the band at 3740 cm^{-1} (associated with termi-

Table 1

Composition and textural properties of the inorganic supports.

Support	Si/Al ^a	$V_{\text{pore}} [\text{cm}^3 \text{g}^{-1}]^b$	$V_{\text{micro}} [\text{cm}^3 \text{g}^{-1}]^c$	$S_{\text{meso}} [\text{m}^2 \text{g}^{-1}]^c$	$S_{\text{BET}} [\text{m}^2 \text{g}^{-1}]^d$
P	26	0.24	0.14	62	378
H	23	0.46	0.11	153	453
HW	26	0.46	0.13	171	497
MCM-41	65	1.15	0.00	927	927

^a Determined by EDX.

^b Measured V_{ads} at $p/p_0 = 0.98$.

^c *t*-plot method.

^d BET method.

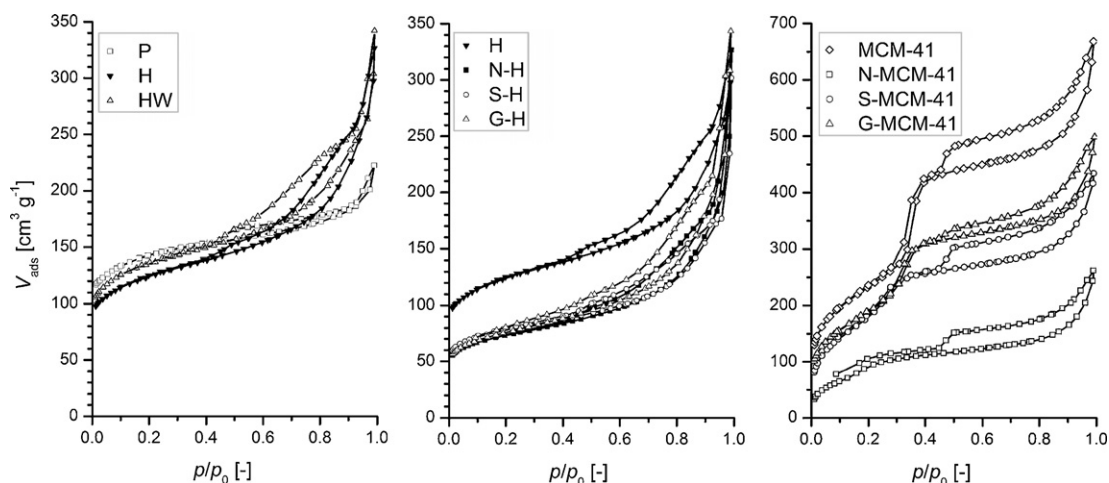


Fig. 2. Comparison of the textural properties of the unfunctionalized P, H, and HW zeolites (left), and of the N-, S-, and G- organic-modified HW zeolite (center) and MCM-41 (right) supports.

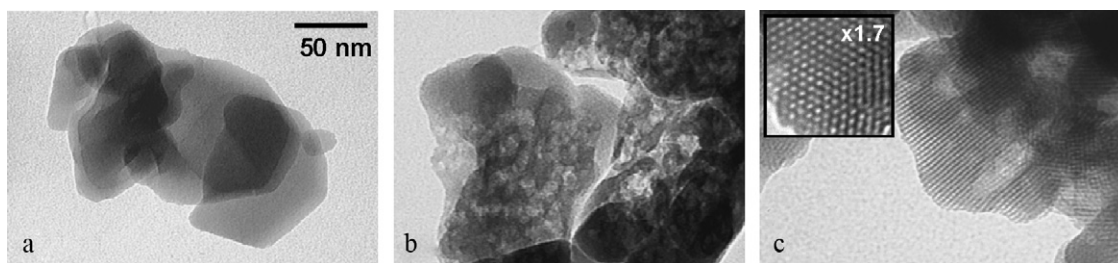


Fig. 3. TEM micrographs comparing the macrostructure and porosity of (a) the P, and (b) H zeolite, and (c) MCM-41 supports. Scale bar applies to all images.

nal silanol groups) and a decrease in the intensity of the broad band at 3490 cm^{-1} (associated with the presence of framework imperfections e.g. silanol nests) is observed on alkaline treatment of the parent zeolite, as expected [11]. Silanization leads to complete loss of the band at 3740 cm^{-1} , confirming reaction of the

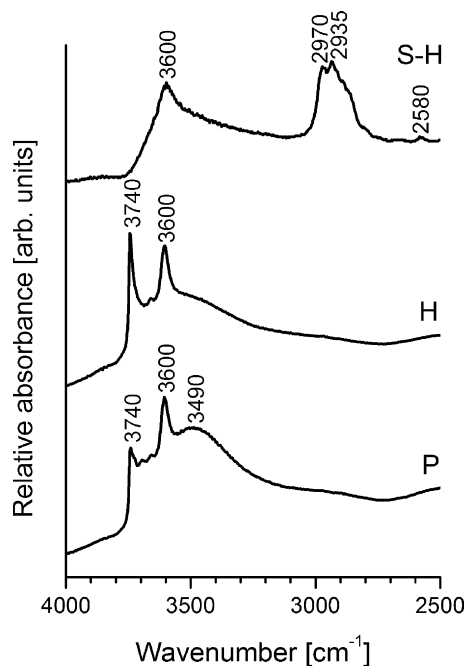


Fig. 4. Observation of the formation and reaction of silanol groups on alkaline treatment of P zeolite and on silanization of the resulting H zeolite with thiol-terminated alkoxysilane (S-H).

silanol groups. Additional bands due to thiol (2580 cm^{-1}) and alkyl ($2850\text{--}3000\text{ cm}^{-1}$) groups confirm the organic modification of the zeolite. No variation in intensity of the band at 3600 cm^{-1} is observed indicating that the Brønsted sites in the zeolite do not partake in the reaction.

The N_2 adsorption isotherms of the N-, S-, and G-modified H and MCM-41 samples are shown in Fig. 2 (corresponding textural parameters found in Supporting Information, Table S1). Although the form of the isotherms remains similar, the total N_2 uptake is clearly reduced upon support modification resulting in a decrease in V_{pore} , S_{BET} , S_{meso} , and V_{micro} in all cases. The S_{meso} of the surface-functionalized H and HW zeolites, however, remained more than double that of the unfunctionalized P zeolite in all cases. The largest variation in S_{meso} was observed for N-MCM-41, which dropped to $S_{\text{meso}} = 274\text{ m}^2\text{ g}^{-1}$. It is interesting to note that although the glutaraldehyde is not expected to interact covalently with the unfunctionalized (alumino-)silicate supports it remains present following support degasification (453 K, 16 h) and also results in significant changes in the support textural properties. Due to the smaller size of glutaraldehyde, a larger drop in V_{micro} compared with S_{meso} is observed, strongly suggesting that it is present in the zeolite micropores.

3.3. Enzyme immobilization

Enzyme immobilization was undertaken by suspension of the potential support material in buffered enzyme-containing solution of known pH and concentration. The properties of the two commercial lipases studied (AS and AK), are summarized in Table 2. A representative structure of a lipase enzyme derived from *Burkholderia cepacia*, in an open configuration in which the polar surface groups are colored blue, may be seen in Fig. 1 [54]. As

Table 2

Properties of the lipase enzymes studied according to manufacturers' specifications.

Lipase ^a	Biological source	pH _{opt} ^b	T _{opt} [K] ^c	p _{iso} ^d	A ≥ [U g ⁻¹] ^e	L [wt.%] ^f	C [wt.%] ^g	N [wt.%] ^g
AS	<i>Aspergillus niger</i>	6	318	4.1	12,000	89	39.8	3.9
AK	<i>Pseudomonas fluorescens</i>	8	328	–	20,000	95	20.7	1.7

^a Manufacturers code.^b Optimal operating pH.^c Optimal operating temperature.^d Iso-electric point.^e Lipolytic activity.^f Lipase content, L, determined by the Bradford method.^g C and N contents determined by elemental analysis.

each enzyme and each support has its own characteristic properties (e.g. isoelectric point, stability range, surface composition, and structure), which may be influenced by factors such as the pH, ionic strength, and temperature used, the conditions chosen for immobilization may have a great impact on the loadings achieved.

In order to determine the relative activities of immobilized versus free enzymes, it is necessary to estimate the enzyme content of the supported biocatalysts. The accurate assessment of the amount of enzyme loaded onto a given support material is non-trivial. Several strategies have been reported including both direct,

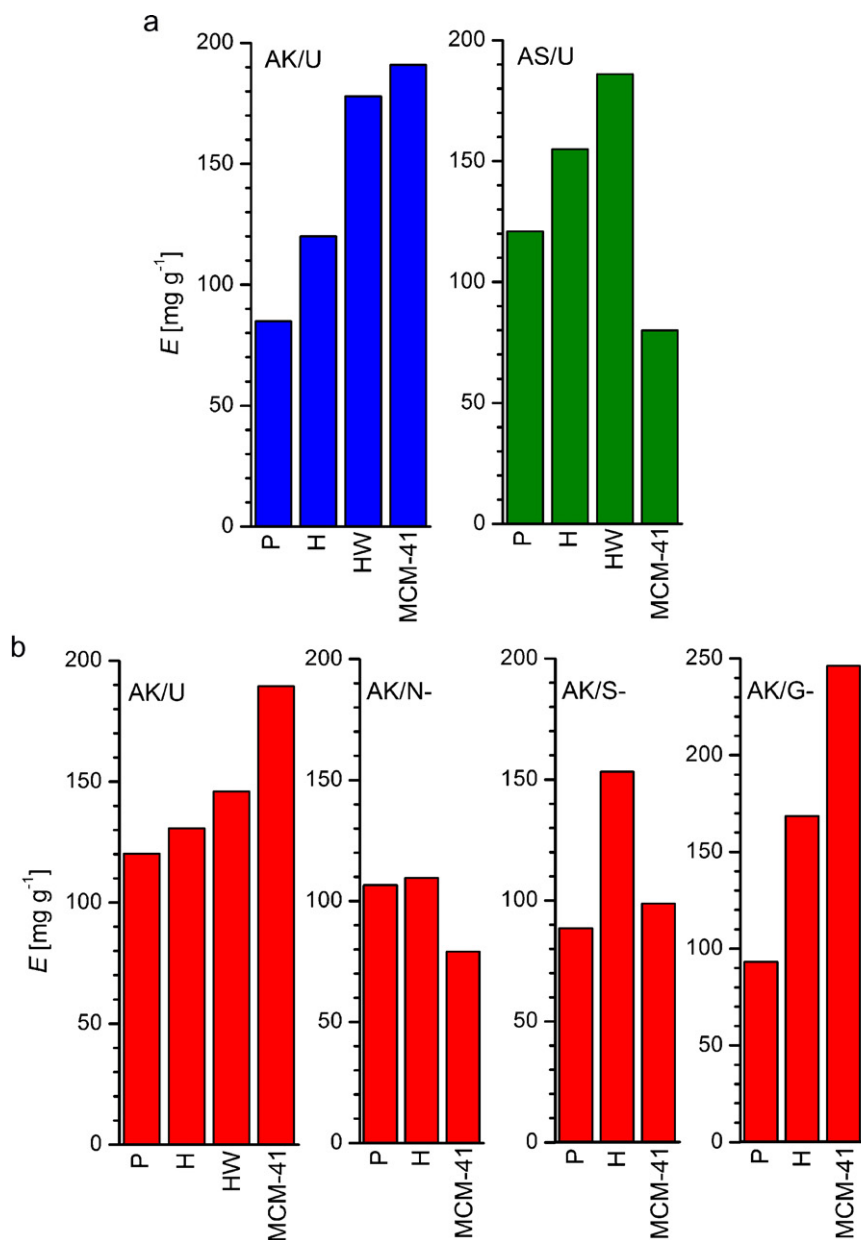


Fig. 5. Comparison of the enzyme uptakes (E) of lipase AK and AS enzymes on P, H, HW, and MCM-41 supports before (U) and after (N- or S-) functionalization estimated by (a) direct elemental analysis and (b) indirect Bradford method.

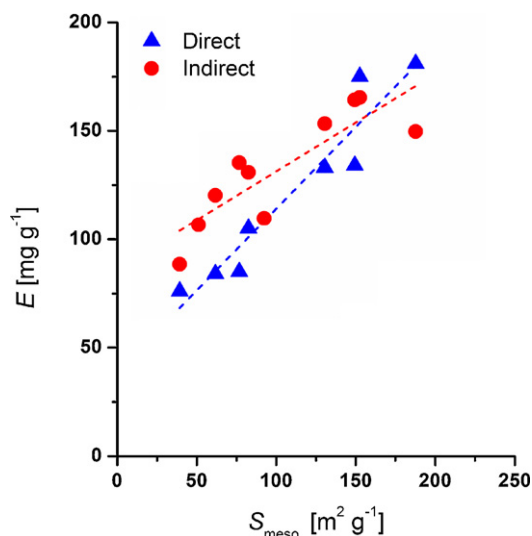


Fig. 6. Relationship between enzyme uptake and mesoporous surface area for the immobilization of lipase AK on unmodified and S- or N-functionalized P, H, HW zeolite-based supports estimated by direct (elemental analysis) and indirect (Bradford) methods.

in which the additional organic component incorporated in the support is measured (e.g. by thermogravimetry [55] or elemental analysis [56]), and indirect, in which the variation in enzyme concentration in solution is measured before and after immobilization (e.g. by the Bradford [55,57] or Lowry [58] methods or by variation in the enzymatic activity [59]).

3.3.1. Direct method

Based on the expected enzyme composition to the enzyme loading of the biocatalyst was estimated by elemental analysis (although the enzyme purity should be taken into account). Comparison of the wt.% of C or N following lipase immobilization indicates that the relative enzyme uptake is dependent on the enzyme studied (Fig. 5a). For lipase AK the enzyme uptake follows the trend MCM-41 > HW > H > P in agreement with the decreasing mesopore surface area. For zeolite based supports a linear relationship is observed between S_{meso} and the amount of enzyme adsorbed, E . This may be clearly seen in Fig. 6 which compares the uptake of lipase AK estimated by direct and indirect methods on zeolites with varying textural properties. A change, HW > H > P > MCM-41, is observed for lipase AS for which the enzyme uptake of MCM-41 was much lower. This suggests that lipase AS is larger than lipase AK and is no longer able to enter the ordered mesopores of MCM-41. Direct methods were most informative for studying the enzyme uptake of the unfunctionalized supports as all of the organic content may be attributed to species adsorbed during enzyme immobilization. A key advantage over the use of indirect methods was the ability to compare adsorption of different lipase enzymes which may have different activities/affinity to the Bradford agent.

3.3.2. Indirect method

The Bradford method is based on the absorbance of the Coomassie brilliant blue dye at 595 nm, which increases on complexation with protein species in solution. Variation in the enzyme content before and after exposure to a given support enables assessment of the amount of enzyme adsorbed. By calibration using a pure gamma globulin standard, the enzyme concentrations in the as-supplied powders were estimated to be AS = 89 wt.%, and AK = 95 wt.%. As lipase AK showed the best response to the Bradford agent, this enzyme was selected for evaluation of support enzyme uptake (E) by this method.

Fig. 5b compares the estimated enzyme loadings obtained with P, H, HW, and MCM-41 supports and with their N-, S-, and G-modified counterparts. A good agreement is observed with the results of elemental analysis, with enzyme uptakes of unmodified supports following MCM-41 > HW > H > P. Use of the Bradford method simplified evaluation of the enzyme uptake of organic modified supports. Organic-functionalized supports typically (with the exception of S-H) exhibited a reduced enzyme uptake with respect to the unmodified frameworks, in agreement with the reduction in S_{meso} . The amount of enzyme adsorbed by N-MCM-41 or S-MCM-41 is significantly lower than of unfunctionalized MCM-41 and of the N-H or S-H zeolites. Although, based on the results of N_2 adsorption, surface-functionalized MCM-41 exhibits a higher S_{meso} than that of the H zeolites, the reduction in mesopore accessibility following surface modification is much more pronounced. Consequently the mono-dimensional mesopores of MCM-41 are less accessible to lipase AK than the larger and interconnected mesopores present in the H zeolites.

An increased enzyme uptake was observed for G-modified H and MCM-41, and a slight reduction in enzyme uptake for the P support. As the interaction of glutaraldehyde with the support is not thought to be covalent, the accuracy of the Bradford method for the determination of enzyme uptake by G-modified supports can be questioned. Dissolution of the cross-linking agent into solution may result in greater reduction in the enzyme concentration due to the formation of cross-linked enzyme aggregates unassociated with the support and thus resulting in over-estimation of the actual enzyme loadings.

Despite all of the considerations mentioned the enzyme uptakes estimated by direct and indirect methods show remarkably close agreement (Fig. 6). Hierarchical zeolites show improved enzyme loading with respect to the P zeolite, which even without significant optimization of the mesopore development is similar to the uptakes observed for MCM-41. For direct methods the question of enzyme purity is clearly important. The organic content introduced by adsorption may not be equivalent to the actual enzyme loading. As the obtainment of pure enzymes typically requires several purification steps the majority of commercially available enzymes are not 100% pure. The complexity of analysis by direct methods increases when studying adsorption on functionalized supports. Determination of the enzyme uptake of organic-modified supports is particularly complex. Although indirect methods appear more useful as they enable direct observation of the enzyme content independent of initial purity two important factors need to be addressed: (a) reduction in enzyme content on exposure to the support may purely be attributed to adsorption and not due to enzyme denaturation on contact with the support; (b) that the enzyme response to the measurement method (e.g. Bradford reagent) is correctly determined. In addition a systematic approach to extraction and subsequent dilution of enzyme-containing solution is essential in order to avoid enzyme losses during these steps.

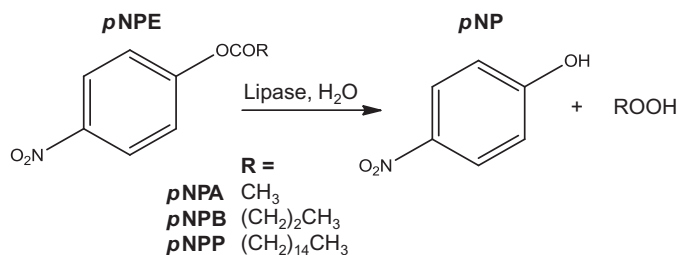
4. Application in biocatalysis

For industrial applications apart from knowledge of the enzyme loading, the catalytic activity and catalyst recyclability are ultimately more important criterion during the assessment of potential supports. Achievement of high enzyme loadings may be fruitless if the supported enzyme is deactivated either due to conformational changes/restriction upon immobilization or due to steric inaccessibility of the active site [60].

4.1. Activity

The activity of the resulting immobilized lipase biocatalysts was screened spectroscopically following the hydrolysis of the

p-nitrophenyl esters (*p*NPEs), a method widely established in the literature as an assay of lipase activity (Eq. (1)) [61–64]. This reaction is particularly useful as the kinetics may be followed quantitatively by UV–vis spectroscopy with no selectivity issues. The *p*NPEs exhibit a single absorbance in the 250–300 nm range, whose position is dependent on the identity of the ester. The *p*NP product showed two absorbance bands at 320 and 405 nm, respectively, indicating the presence of the *p*-nitrophenolate anion under the conditions studied. Biocatalyst activities may be evaluated in either aqueous or, following product extraction, organic phase [65].



Typically the extent of reaction is monitored by studying the increase in the concentration of the *p*NP product. As some (microporous) supports were found to adsorb the reacting species to a greater extent leading to reduction in the absorbance of the substrate and product, herein the preferred method for estimation of the conversion, *X* [%], achieved during catalytic screening was by comparison of the relative intensities of the *p*NPE substrates (e.g. *p*NPB = 273 nm) and *p*NP product (405 nm) absorbance bands. The reaction pH was found to have a significant influence on the rate of spontaneous ester hydrolysis. A marked increase in the rate of spontaneous hydrolysis was observed for $\text{pH} \geq 7$ (with 100% conversion observed within 30 min) and consequently it was impossible to decouple the rate of spontaneous hydrolysis from the rate of enzyme catalyzed hydrolysis. Results presented in this work were undertaken at pH 6 in order to minimize the rate of spontaneous ester hydrolysis (typically less than 15%).

Before screening of the biocatalyst, the activities of the unsupported enzymes and individual supports were assessed. Due to the higher relative ester stability (with respect to spontaneous hydrolysis) and to the fewer steps required, initial screening of catalytic activity was undertaken with *p*-nitrophenyl butyrate (*p*NPB) in the aqueous phase. Both lipase enzymes were active for the hydrolysis of the *p*NPB (Fig. 7a). Large changes are observed in the UV–vis with respect to those observed by spontaneous hydrolysis (i.e. for the blank) with the activity of lipase AS showing very similar activity to lipase AK, for this assay in the unsupported form. No significant *p*NPB hydrolysis was observed in the presence of any of the support materials (Fig. 7b). Small variations in the absorbance of the ester substrate (I_{273}) were attributed to differing extents of adsorption between supports, which was greatest for the organic-modified supports.

For the supported biocatalysts slightly higher activities were observed for AK than for AS enzymes. The relative activities of the biocatalysts exhibited good correlation with the estimated enzyme loadings. This may be seen qualitatively by comparison of the UV–vis spectra resulting from catalytic screening of supported AS, which shows greater conversion of the ester for the H zeolite than the P zeolite (Fig. 7c). A quantitative comparison of the degree of conversion with respect to the support enzyme uptake is shown in Table 3. The relative activity follows the trend $\text{MCM-41} > \text{HW} > \text{H} > \text{P}$.

Enzymes supported on N-, S-, and G-modified supports show differing initial activities, but lipase AK remained more active than lipase AS in all cases. Despite the lower estimated enzyme loadings,

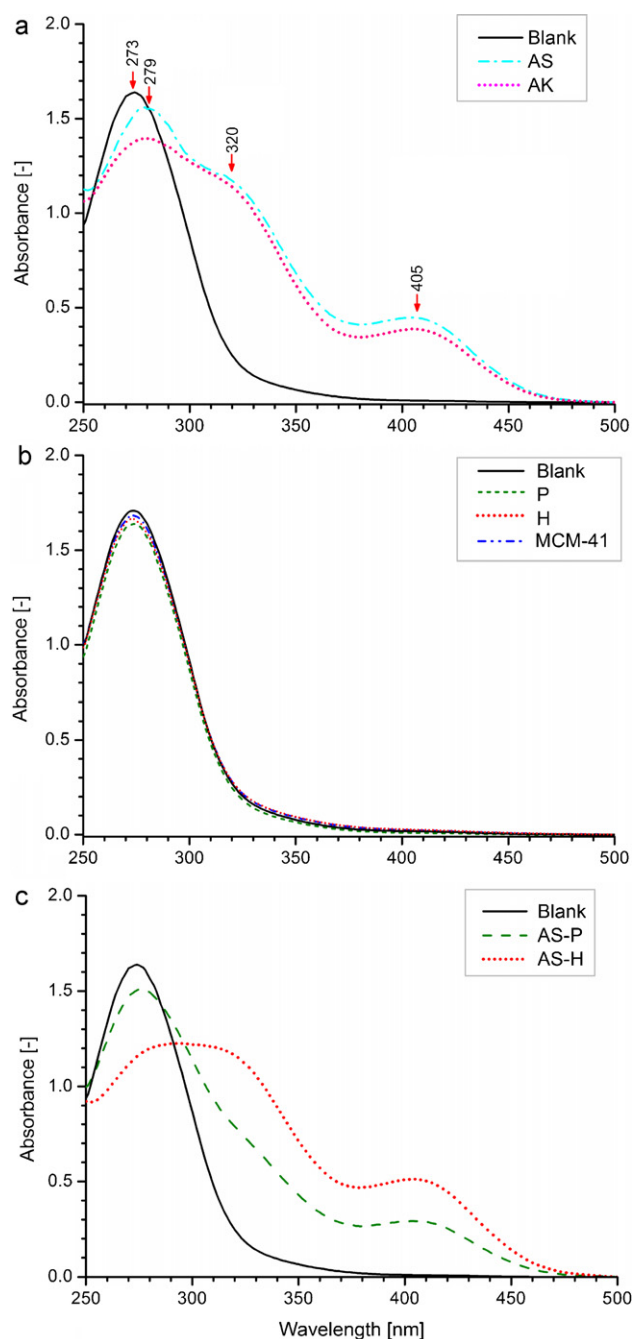


Fig. 7. Comparison of the activity of (a) the unsupported AS and AK enzymes, (b) the P, H and MCM-41 supports and (c) the AS-P and AS-H supported lipase biocatalysts for the hydrolysis of *p*NPB (Eq. (1)).

Table 3

Comparison of the enzyme uptakes, *E*, with the initial activities of AS and AK enzymes immobilized on P, H, HW, and MCM-41 supports.

Support	AS		AK	
	<i>E</i> [mg g ⁻¹] ^a	<i>X</i> [%] ^b	<i>E</i> [mg g ⁻¹] ^a	<i>X</i> [%] ^b
P	121	26	85	79
H	155	36	120	82
HW	186	51	178	94
MCM-41	80	50	191	100

^a Estimated from the results of elemental analysis.

^b % of conversion, *X*, of *p*NPB measured at *t* = 30 min.

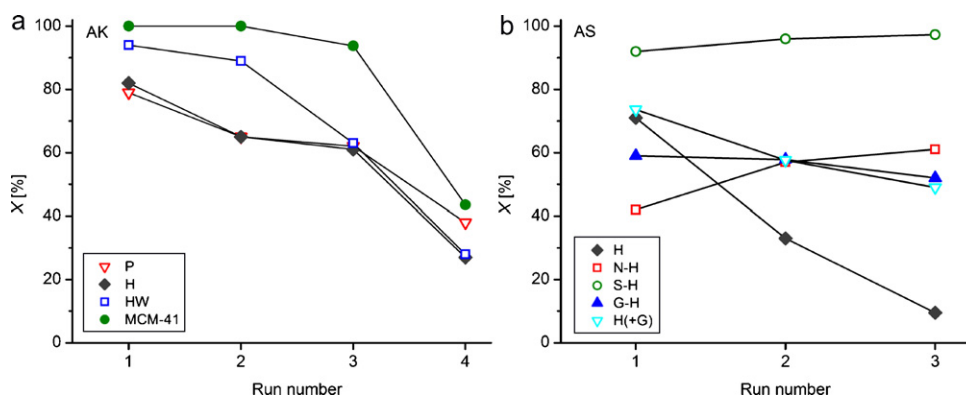


Fig. 8. Comparison of the average retention of activity on catalytic recycling of (a) lipase AK supported on the unmodified P, H, HW, and MCM-41 supports and (b) lipase AS supported on the N-, S- and G-modified H zeolite compared with that of the unfunctionalized H and H(+G) in which glutaraldehyde was added simultaneously to enzyme immobilization.

lipases immobilized on S-modified supports exhibit the highest activities in all cases ($X=100$ and 92% for AK and AS on S-H, respectively). G- and N-modified supports show lower initial activities, in most cases lower than those of the respective unmodified supports.

4.2. Recyclability

The influence of the support textural and surface properties on the biocatalyst recyclability was investigated by studying the variation in degree of conversion during consecutive runs (Fig. 8). Independent of the initial enzyme loading, rapid loss of enzymatic activity is observed for all of the unfunctionalized supports on application in aqueous phase catalysis. It is likely that the loss of activity results from enzyme leaching in agreement with the findings of previous works describing immobilization by adsorption on purely inorganic supports [33]. The mesoporous MCM-41 and HW supports show the slowest rates of catalyst deactivation (demonstrated for lipase AK in Fig. 8a).

Preliminary results of the catalytic recyclability of organic-modified zeolites indicate significant improvements in activity retention compared with that of enzymes supported on unmodified zeolites. A comparison of the retention of activity of AS immobilized on H, N-H, S-H, G-H, and H + G supports for three consecutive catalytic runs is shown in Fig. 8b. In contrast to the unfunctionalized H support, the activities of AS enzymes immobilized on the functionalized supports and those which were treated with glutaraldehyde either prior or during enzyme immobilization show a much higher retention. Remarkably, the activity of S-functionalized supports remained close to 100% for AS supported on S-H over three cycles. The activity of N-H, although initially lower than that of the unfunctionalized H based biocatalyst, was also retained. In fact, the activity showed a slight increase. This could be a result of increased product partitioning by the N-functionalized biocatalysts leading to an artificial enhancement in the product concentration on repeated cycling. Alternatively, it could be an indication of progressive weakening of the enzyme-support interaction leading to increased accessibility to the active site. Biocatalysts prepared with treatment of glutaraldehyde during enzyme immobilization showed slightly higher initial activities than those where glutaraldehyde was introduced by pretreatment prior to immobilization. It is possible that application during treatment leads to the formation of cross-linked enzyme aggregates in solution which may adsorb to the support surface. The loss of such species could explain the slightly higher relative activity loss observed for the H zeolite for which enzyme adsorption was undertaken in the presence of glutaraldehyde.

5. Mesoporous zeolites: suitable hosts for large active species?

Much attention has been drawn to the employment of ordered mesoporous materials for enzyme immobilization. The alkaline treatment and subsequent mild acid washing of purely microporous zeolites provides a versatile route for the controlled introduction of intracrystalline mesoporosity with tailored compositional properties. Furthermore, the textural properties and surface composition of the hierarchical zeolites may be modified by functionalization of the silanol groups present at the mesopore surface. Our results show that provided the mesopore is accessible to the guest species (in this case different lipase enzymes) then the uptake or large guests (which are unable to enter the micropores) increases proportionally with the mesoporous surface area of the host.

Surface functionalization leads to a reduction in the mesoporous surface area and directly impacts the amount of enzyme adsorbed. For ordered mesopores silicas depending on the pore size there is a critical point at which the mesopore becomes inaccessible on further reduction of mesopore size and a step change in the guest uptake is observed (as seen for the uptake of lipase AK on S-/N-MCM-41). Due to the topographical non-uniformity of the zeolite mesopores no such marked change in adsorption properties is observed. H zeolites modified by silanization exhibited uptakes greater than or comparable to those of similarly modified MCM-41. The reduced lipase uptake by surface functionalized MCM-41 supports was also reflected by a reduction of the initial biocatalytic activity.

During catalytic screening the initial activities of the supported enzymes are most strongly influenced by the enzyme uptake during immobilization which shows greatest dependence on the enzyme-accessible surface area. The increase in enzyme adsorption observed for acid washed mesoporous zeolites is thought to be predominantly connected to the increased accessible surface area and the presence of extra framework aluminum species did not significantly influence either the enzyme uptake or biocatalyst activity. No significant mesopore-related enhancement in the retention of enzymes immobilized on unfunctionalized supports was observed on application confirming that the enzyme-support interactions (e.g. ionic, van der Waals, hydrogen bonding, hydrophobic) are insufficient to prevent enzyme leaching on application for aqueous phase catalysis, and that physical protection does not reduce desorption significantly under these conditions (Fig. 7a).

Surface functionalization improves retention of activity. As the enzyme uptake is not significantly increased for the organic modified supports this is thought to be due to the formation of

stronger enzyme–support interactions and improved stabilization with respect to enzyme leaching. For the lipase enzymes studied thiol functionalized surfaces are found to be most promising, showing higher degrees of conversion in ester hydrolysis in all cases. Improvements in enzyme immobilization have previously been reported for thiol terminated surfaces [47]. This has been related to improved enzyme stability due to increased surface hydrophobicity or due to interaction of the thiol groups with –SH or other S-containing groups present on the enzyme surface (e.g. chemisorption by the formation of disulfide bridges [66]). Many lipase enzymes are also known to require interfacial activation in order for the active site to be accessible. ‘Hyperactivation’ of the enzyme (i.e. where the supported enzyme adopts a conformation in which the active site is exposed) is another common explanation [49,67]. No such activity enhancement was observed for lipases immobilized on amine functionalized supports or for those modified with glutaraldehyde whose activities were found to reflect the amount of supported enzyme.

6. Conclusions

Mesopores present in hierarchical zeolites prepared by desilication are accessible to lipase enzymes and have tunable surface properties, extending their potential as hosts to larger guest species. Enhancement in the enzyme uptake and biocatalytic activity with respect to purely microporous zeolites may be directly correlated to the increased mesoporous surface area. Surface functionalization by silanization or the employment of the enzyme cross-linking agent glutaraldehyde was found to be imperative in order to reduce loss of activity due to enzyme desorption on application in the aqueous phase. The disorder and interconnectivity of mesopores present in hierarchical zeolites were found to be beneficial in improving mesopore accessibility post-functionalization. Work to improve understanding of the enzyme–support interactions in surface functionalized supports and to explore the potential enhancement in performance of biocatalysts based on hierarchical porous zeolites in organic medium is in progress. These supports are expected to offer attractive prospects for more complex catalyst designs such as for the co-immobilization of different enzymatic or cofactor species with controlled reaction environments.

Appendix A. Supplementary data

Supplementary data associated with this article can be found, in the online version, at doi:10.1016/j.cattod.2010.10.058.

References

- [1] A.D. McNaught, A. Wilkinson (Eds.), *Compendium of Chemical Terminology*, Blackwell Science, Oxford, 1997, IUPAC 2nd revised ed.
- [2] G.W. Xing, X.W. Li, G.L. Tian, Y.H. Ye, *Tetrahedron* 56 (2000) 3517.
- [3] A.P.V. Gonçalves, J.M. Lopes, F. Lemos, F. Ramôa Ribeiro, D.M.F. Prazeres, J.M.S. Cabral, M.R. Aires-Barros, *J. Mol. Catal. B: Enzym.* 1 (1996) 53.
- [4] Y.Y. Hu, Y.H. Zhang, N. Ren, Y. Tang, *J. Phys. Chem. C* 113 (2009) 18040.
- [5] Y. Zhang, X. Want, W. Shan, B. Wu, H. Fan, X. Yu, Y. Tang, P. Yang, *Angew. Chem. Int. Ed.* 44 (2005) 615.
- [6] A. Corma, V. Fornes, F. Rey, *Adv. Mater.* 14 (2002) 71.
- [7] J. Pérez-Ramírez, C.H. Christensen, K. Egeblad, C.H. Christensen, J.C. Groen, *Chem. Soc. Rev.* 37 (2008) 2530.
- [8] M. Hartmann, *Angew. Chem. Int. Ed.* 43 (2004) 5880.
- [9] D.H. Lee, M. Choi, B. Woo, R. Ryoo, *Chem. Commun.* (2009) 74.
- [10] M. Ogura, S. Shinomiya, J. Tateno, Y. Nara, E. Kikuchi, M. Matsukata, *Chem. Lett.* (2000) 882.
- [11] J.C. Groen, L.A.A. Peffer, J.A. Moulijn, J. Pérez-Ramírez, *Chem. Eur. J.* 11 (2005) 4933.
- [12] F. Thibault-Starzyk, I. Stan, S. Abelló, A. Bonilla, K. Thomas, C. Fernández, J.P. Gilson, J. Pérez-Ramírez, *J. Catal.* 264 (2009) 11.
- [13] D. Vasić-Rački, in: A. Liese, K. Seelbach, C. Wandrey (Eds.), *Industrial Biotransformations*, vol. 1, Wiley-VCH, Weinham, 2006, pp. 1–36.
- [14] L. Michaelis, M. Ehrenreich, *Biochem. Z.* 10 (1908) 283.
- [15] Tate and Lyle, Ltd., H.C.S. de Whalley, British patent No. 564270, 1944.
- [16] R.A. Messing, FR patent No. 2001336, 1969.
- [17] I. Chibata, *Adv. Mol. Cell Biol.* 15A (1996) 151.
- [18] K. Mosbach, *FEBS Lett.* 62 (1976) E80.
- [19] D. Thomas, *Trends Biotechnol. Sci.* (1979) N207.
- [20] A.M. Klivanov, *Anal. Biochem.* 93 (1979) 1.
- [21] C.A. White, J.F. Kennedy, *Enzyme Microb. Technol.* 2 (1980) 82.
- [22] W. Hartmeier, *Trends Biotechnol.* 6 (1985) 149.
- [23] R.A. Sheldon, *Adv. Synth. Catal.* 349 (2007) 1289.
- [24] U. Hanefeld, L. Gardossi, E. Magner, *Chem. Soc. Rev.* 38 (2009) 453.
- [25] T. Hudlicky, J.W. Reed, *Chem. Soc. Rev.* 38 (2009) 3117.
- [26] J. Ge, D. Lu, Z. Liu, Z. Liu, *Biochem. Eng. J.* 44 (2009) 53.
- [27] J.F. Diaz, K.J. Balkus, *J. Mol. Catal. B: Enzym.* 2 (1996) 115.
- [28] C.H. Lee, J. Lang, C.W. Yen, P.C. Shih, T.S. Lin, C.Y. Mou, *J. Phys. Chem. B* 109 (2005) 12277.
- [29] A. Macario, A. Katovic, G. Giardano, L. Forni, F. Carloni, A. Filippini, L. Setti, *Stud. Surf. Sci. Catal.* 155 (2005) 381.
- [30] I.I. Slowing, B.G. Trewyn, V.S.Y. Lin, *J. Am. Chem. Soc.* 129 (2007) 8845.
- [31] S. Hudson, J. Cooney, E. Magner, *Angew. Chem. Int. Ed.* 47 (2008) 8582.
- [32] C.H. Lee, T.S. Lin, C.Y. Mou, *Nano Today* 4 (2009) 165.
- [33] M. Hartmann, D. Jung, *J. Mater. Chem.* 20 (2010) 844.
- [34] C. Baerlocher, L.B. McCusker, D.H. Olson, *Atlas of Zeolite Framework Types*, 6th ed., Elsevier, 2007.
- [35] F.N. Serralha, J.M. Lopes, F. Lemos, D.M.F. Prazeres, M.R. Aires-Barros, J.M.S. Cabral, F. Ramôa-Ribeiro, *J. Mol. Catal. B: Enzym.* 4 (1998) 303.
- [36] T. Ke, A.M. Klivanov, *J. Am. Chem. Soc.* 121 (1999) 3334.
- [37] K.M. Koeller, C.H. Wong, *Nature* 409 (2001) 232.
- [38] A. Schmid, J.S. Dordick, B. Hauer, A. Kiener, M.G. Wubbolts, B. Witholt, *Nature* 209 (2001) 258.
- [39] M. Kim, J. Kim, J. Lee, H. Jia, H.B. Na, J.K. Youn, J.H. Kwak, A. Dohnalkova, J.W. Grate, P. Wang, T. Hyeon, H.G. Parl, H.N. Chang, *Biotechnol. Bioeng.* 96 (2006) 210.
- [40] X. Feng, G.E. Fryxell, L.Q. Wang, A.Y. Kim, J. Liu, K.M. Kemner, *Science* 276 (1997) 923.
- [41] J.C. Groen, W. Zhu, S. Brouwer, S.J. Huynink, F. Kapteijn, J.A. Moulijn, J. Pérez-Ramírez, *J. Am. Chem. Soc.* 129 (2007) 355.
- [42] S. Abelló, A. Bonilla, J. Pérez-Ramírez, *Appl. Catal. A* 364 (2009) 191.
- [43] J.C. Groen, T. Bach, U. Ziese, A.M. Paulaime-van Donk, K.P. de Jong, J.A. Moulijn, J. Pérez-Ramírez, *J. Am. Chem. Soc.* 127 (2005) 10792.
- [44] C. Fernandez, I. Stan, J.-P. Gilson, K. Thomas, A. Vicente, A. Bonilla, J. Pérez-Ramírez, *Chem. Eur. J.* 16 (2010) 6224.
- [45] H. Naono, M. Hakuman, T. Tsunehisa, N. Tamura, K. Nakai, *J. Colloid Interface Sci.* 224 (2000) 358.
- [46] R. Schmidt, M. Stocker, E. Hansen, D. Akporiaye, O.H. Ellestad, *Micropor. Mater.* 3 (1994) 443.
- [47] H.H.P. Yiu, P.A. Wright, *J. Mater. Chem.* 15 (2005) 3690.
- [48] P. Reis, T. Witula, K. Holmberg, *Micropor. Mesopor. Mater.* 110 (2008) 355.
- [49] J.M. Palomo, G. Fernandez-Lorente, C. Mateo, R.L. Segura, C. Ortiz, R. Fernandez-Lafuente, J.M. Guisan, in: J.M. Guisan (Ed.), *Immobilization of Enzymes and Cells*, 2nd ed., Humana Pr. Inc., Totowa, 2006, p. 143.
- [50] B. Dragoi, E. Dumitriu, *Acta Chim. Slov.* 55 (2008) 277.
- [51] S. Mandal, D. Roy, R.V. Chaudhari, M. Sastry, *Chem. Mater.* 16 (2004) 3714.
- [52] K. Mukhopadhyay, S. Phadtare, V.P. Vinod, A. Kumar, M. Rao, R.V. Chaudhari, M. Sastry, *Langmuir* 19 (2003) 3858.
- [53] G.N. Le Fevre, B.A. Saville, *US. Patent* 5998183, 1999.
- [54] J.D. Schrag, Y. Li, M. Cygler, D. Lang, T. Burgdorf, H.J. Hecht, R. Schmid, D. Schomburg, T.J. Rydel, J.D. Oliver, L.C. Strickland, C.M. Dunaway, S.B. Larson, J. Day, A. McPherson, *Structure* 5 (1997) 187.
- [55] D. Moelans, P. Cool, J. Baeyens, E.F. Vansant, *Catal. Commun.* 6 (2005) 307.
- [56] Y. Han, S.S. Lee, J.Y. Ying, *Chem. Mater.* 18 (2006) 643.
- [57] X. Wang, P. Dou, P. Zhao, C. Zhao, Y. Ding, P. Xu, *ChemSusChem* 2 (2009) 947.
- [58] S. Salis, E. Sanjust, V. Solinas, M. Monduzzi, *Biocatal. Biotransform.* 23 (2005) 381.
- [59] R.M. Blanco, P. Terreros, M. Fernandez-Perez, C. Otero, G. Diaz-Gonzalez, *J. Mol. Catal. B: Enzym.* 30 (2004) 83.
- [60] A. Macario, G. Giordano, L. Setti, A. Parise, J.M. Campelo, J.M. Marinas, D. Luna, *Biocatal. Biotransform.* 25 (2007) 328.
- [61] L. Costa, V. Brissos, F. Lemos, F. Ramôa Ribeiro, J.M.S. Cabral, *Appl. Spectrosc.* 62 (2008) 932.
- [62] A. Galarneau, M. Mureseanu, S. Atger, G. Renard, F. Fajula, *New. J. Chem.* 30 (2006) 562.
- [63] L. Costa, V. Brissos, F. Lemos, F. Ramôa Ribeiro, J.M.S. Cabral, *Bioprocess. Biosyst. Eng.* 31 (2008) 323.
- [64] L. Costa, V. Brissos, F. Lemos, F. Ramôa Ribeiro, J.M.S. Cabral, *Bioprocess. Biosyst. Eng.* 32 (2009) 53.
- [65] J. Yang, Y. Koga, H. Nakano, T. Yamane, *Protein Eng.* 15 (2002) 147.
- [66] H.P. Humphrey, P.A. Wright, N.P. Botting, *J. Mol. Catal. B: Enzym.* 15 (2001) 81.
- [67] A. Bastida, P. Sabuquillo, P. Armisen, R. Fernandez-Lafuente, J. Hugué, J.M. Guisan, *Biotechnol. Bioeng.* 58 (1997) 486.